Interactions of equatorial winds in super-Eddington stellar sources

L. Abaroa[1], P. Sotomayor Checa[1,2] & G.E. Romero[1,2]

[1] *Facultad de Cs. Astronómicas y Geofísicas, UNLP, Argentina*
[2] *Instituto Argentino de Radioastronomía, CONICET–CICPBA–UNLP, Argentina*

Contact / leandroabaroa@gmail.com

Resumen / Los objetos compactos con tasas de acreción súper-Eddington lanzan vientos y *jets* poderosos. En el sistema binario el *jet* interactúa con el viento del disco. Un *jet* extremadamente poderoso deflecta el viento hacia fuera del sistema produciendo un flujo ecuatorial supersónico. Esta podría ser la situación del microcuásar galáctico SS433, en el cual se ha encontrado evidencia de un viento ecuatorial por medio de observaciones interferométricas de alta resolución. En este trabajo presentamos resultados preliminares de estimaciones cuantitativas de la radiación esperada, producto de la interacción entre el viento ecuatorial generado por el *jet* y una estrella donante de gran luminosidad sin vientos (p.ej. una estrella de Población III). Los resultados son de interés para la comprensión de fuentes ultraluminosas de rayos X y otros acretores súper-Eddington en el universo temprano.

Abstract / Compact objects accreting at super-Eddington rates launch powerful winds and jets. The jet interacts with the wind of the disk. A powerful jet pushes the wind sidewards producing a supersonic equatorial outflow. Such a situation might be the case in the well-known super-accreting Galactic microquasar SS433, where the existence of an equatorial wind has been revealed by high-resolution radio observations. In this work, we present preliminary results of quantitative estimates of the expected radiation from the interaction between a jet-induced equatorial wind and a very luminous donor star with weak or null winds (e.g. a PopIII star). The results are of interest for understanding ultraluminous X-ray sources and other super-Eddington accretors in the early universe.

Keywords / accretion, accretion disks — radiation mechanisms: non-thermal — stars: black holes — stars: winds, outflows — X-rays: binaries

1. Introduction

The most important parameter in accretion disk theory is the critical accretion rate defined as

$$\dot{M}_{\mathrm{crit}} \equiv \eta\, \dot{M}_{\mathrm{Edd}} = \frac{L_{\mathrm{Edd}}}{c^2} \approx 1.4 \times 10^{17} \frac{M}{M_\odot}\ \mathrm{g\,s^{-1}}, \quad (1)$$

where L_{Edd} is the Eddington luminosity. This is the rate necessary to stop the accretion by radiation pressure.

Depending on how the accretion rate relates to the critical rate, we can define three basic kinds of regimes. If the accretion rate is very low ($\dot{M} \ll \dot{M}_{\mathrm{crit}}$), the disk is geometrically-thick and supposed to be in the optically-thin advection dominated state (Narayan & Yi, 1994). In the case of a sub-critical regime ($\dot{M} \lesssim \dot{M}_{\mathrm{crit}}$), the disk is geometrically-thin and optically-thick; this is the well-known standard disk described by Shakura & Sunyaev (1973). For a super-critical accretion rate ($\dot{M} \gg \dot{M}_{\mathrm{crit}}$) the disk becomes geometrically and optically-thick (Abramowicz et al., 1980; Fukue, 2004).

We are interested in this latter case, where the disk undergoes a transition from sub-critical to super-critical regime at a certain radius. We can find this transitional or critical radius by comparing the vertical components of the radiative and gravity forces over an element of mass of the disk, obtaining $r_{\mathrm{cr}} \approx 4\dot{m}r_{\mathrm{g}}$, where $\dot{m}$ is the accretion rate in units of $\dot{M}_{\mathrm{crit}}$, and r_{g} is the gravitational radius.

The disk is separated in two regions: an inner disk ($r < r_{\mathrm{crit}}$) in an ADAF (advection-dominated accretion flow) state, and an outer standard disk ($r > r_{\mathrm{crit}}$) dominated by radiation pressure. In the inner disk, the radiative force overcomes gravity and a wind should be produced.

In this work, we adopt the hypothesis of Fukue (2004), that the mass accretion rate in the inner disk is regulated just at the critical rate with the help of the wind mass-loss. Hence, the accretion rate has a dependence with the radius in the inner disk, $\dot{M}(r)$, and the disk undergoes mass-loss via radiatively-driven winds:

$$\dot{M}_{\mathrm{wind}} = \dot{M}_{\mathrm{input}} - \dot{M}(r). \quad (2)$$

This optically-thick wind should interact with the jet of the system. An extremely powerful jet might push sidewards the wind producing an equatorial flow (Sotomayor Checa et al., submitted). This jet-induced supersonic equatorial wind interacts with the donor star.

In this work, we investigate the effects of the interaction of an equatorial wind with the very luminous star of a microquasar of Population III.

2. Accretion disk

We adopt an accretion rate at the outer region of the disk of $\dot{M}_{\mathrm{input}} = 10^4\ \dot{M}_{\mathrm{crit}}$. We use the semi-analytical model of Fukue (2004) and assume the hypothesis therein, i.e., the accretion rate is regulated just

at the critical rate with the help of the wind mass-loss. There is no net momentum gain/loss associated with the wind.

We apply an hydrodynamical treatment with radiation pressure and use the continuity equation with mass loss. Since the inner disk becomes advection-dominated, in the energy equation the advection heating is given by $Q_{adv} = Q_{vis}^+ - Q_{rad}^- = fQ_{vis}^+$, where f is the advection parameter. The advection process causes the generated energy via viscous dissipation to be restored as entropy of the accreting gas rather than being radiated (Wang & Zhou, 1999). This leads to a jump in some physical quantities at the critical radius depending on the values adopted of the advection and viscous parameters. In our model for the disk, we fix the advection to $f = 0.5$, and adopt a low viscosity, $\alpha = 0.01$.

The plasma is treated as a mono-atomic relativistic ideal gas, with adiabatic coefficient in $\gamma = 4/3$. For these values, we find the following characteristics:

- There is a half-an-order-magnitude jump at the critical radius for the medium scale-height. The geometry of the disk, uniform for $r > r_{crit}$, adopts a radial-dependence for $r < r_{crit}$, reducing its thickness in orders of magnitude near to the event horizon of the black hole.

- The radial drift velocity suffers a jump of nearly one order of magnitude at the critical radius and its radial description changes the slope between the two parts of the disk. In the inner edge of the disk the flow reaches an infall velocity of, approximately, $v_r \approx 10^8$ cm s^{-1}.

- There is a small change in the slope of the effective temperature distribution of the disk at the critical radius, reaching approximately a value of 10^7 K in the inner edge of the disk.

- Since the disk is optically-thick, we assume that it radiates as a blackbody. The maximum luminosity reached is at the order of the Eddington luminosity $\approx 5 \times 10^{39}$ erg s^{-1}. This is shown in Fig. 4.

3. Equatorial wind

An extremely powerful jet pushes sidewards the radiatively driven wind from the accretion disk. We use the relativistic hydrodynamics simulations (RHD) developed by Sotomayor Checa et al. (2021) to characterize this process. In the case of a relative kinetic power between the jet and wind of $L_j = 100 L_w$, the RHD show the formation of a supersonic equatorial wind. This flow could produce shock waves when it interacts with the star.

We apply this model to a Population III star, which is very luminous but has weak or null winds (see e.g. Sotomayor Checa & Romero (2019)). The strong radiation pressure from the star might halt the equatorial wind at a certain stagnation point. This point can be found by equalling the ram pressure from the wind with the radiation pressure from the star, $\rho_w(r_{BH}) v_w^2 = P_{rad}$. This produces an adiabatic down-stream reverse shock, where particles can be accelerated by a first order Fermi process. We define a narrow acceleration region around the stagnation point, with a thickness of
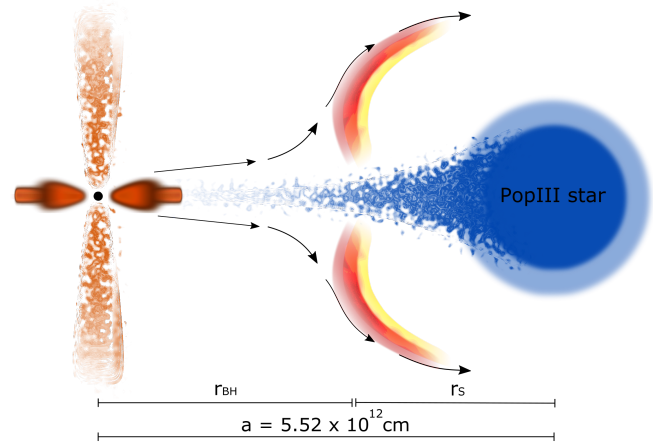

Figure 1: Scheme of the interaction between the equatorial wind and the donor star. The wind stagnates at a r_{BH} distance from the black hole.

$\Delta x_{acc} = 1.2 \times 10^8$ cm, in which the one-zone model is valid. This scenario is represented in Fig. 1.

The cooling rate of the relativistic particles in the one-zone is the sum of the radiative cooling rate and adiabatic losses rate $t_{cool}^{-1} = t_{rad}^{-1} + t_{ad}^{-1}$, while the acceleration rate in the reverse shock is parametrized by the acceleration efficiency. Since the latter is defined as the square of the ratio between shock and light velocities, and shock velocity is $v_s \approx 4v_w/3$ (Lee et al., 1996), we obtain an acceleration mechanism with $\eta_{acc} = 10^{-4}$. If the time-scales of cooling are shorter than those of escape, particles radiate before they escape from the acceleration region. We can find the maximum energy reached by the particles before they escape, by equalling the acceleration and cooling time-scale.

4. Results

4.1. Time scales

We consider only the electrons, since protons escape without cooling from the acceleration region. We estimate the magnetic field at the stagnation point, $B_{sp} = 60$ G, as a fraction of the dipole B_* on the star surface, following Eichler & Usov (1993). We assume a convective escape, i.e., the particles are removed from the acceleration region by the bulk motion of the fluid.

In Fig. 2 the cooling and acceleration time-scales for electrons are represented in logarithmic scale. Particles with energies from 1 MeV to 1 GeV escape before cooling. The inverse Compton (IC) scattering –due to the interaction of the electrons with the stellar radiation field– is the dominant radiative process for energies between 1 and 10 GeV, just in the transition between the Thomson and Klein-Nishina regimes. The cutoff energy is about 10 GeV.

4.2. Particle distribution

We solve the transport equation in the steady state, with an injection power-law distribution of index 2.2
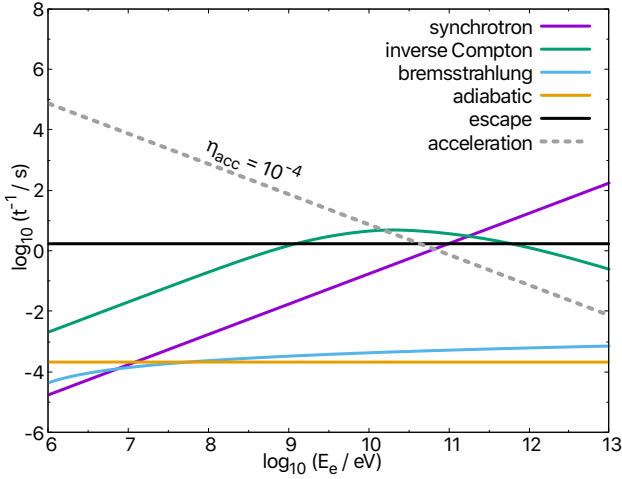
Figure 2: Leptonic cooling time-scales in the acceleration region considering adiabatic and radiative losses. The dominant cooling process is the IC scattering at energies of 1 GeV.
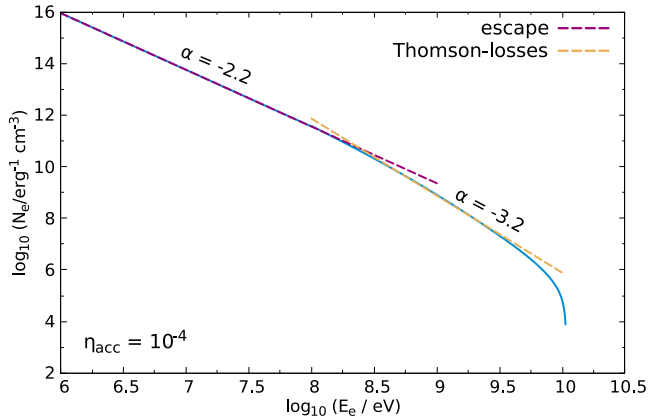

Figure 3: Leptonic particle distribution. At low energies the particle escape dominates, so the spectral index of the distribution does not differ from that of the injection function. At ≈ 100 MeV there is a softening of the spectrum due to Thomson-losses.

and an exponential cutoff. In Fig. 3 the power-law particle spectrum in logarithmic scale shows the dominant escape in the energy range $1 - 100$ MeV (with spectral index 2.2), while Thomson losses dominate the range 100 MeV $- 10$ GeV (steepening the spectral index to 3.2).

4.3. Non-thermal spectral energy distribution

We consider IC scattering and synchrotron radiation for the non-thermal emission. The spectral energy distribution (SED) in Fig. 4 shows a multi-wavelength emission, with a maximum at soft gamma rays, reaching a luminosity of 10^{34} erg s^{-1}. In the range 10^{-2} eV $- 10$ keV the spectrum is dominated by the thermal radiation of the disk, as expected. Non-thermal contributions are
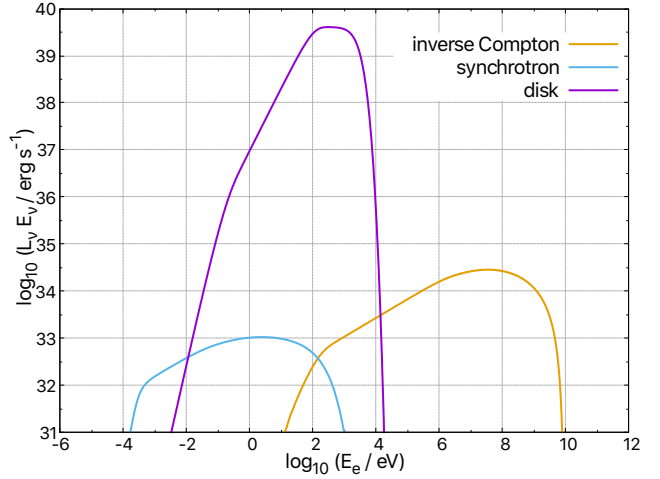

Figure 4: Non-thermal SEDs for the synchrotron and inverse Compton processes. There is a maximum at $E \approx 100$ MeV for the non-thermal emission. In addition, we show the thermal SED for the critical accretion disk.

important at hard X-ray and gamma-ray energies.

Gamma rays with $E > 100$ MeV should be absorbed by $\gamma\gamma$–annihilation in the disk radiation field, and pairs created should be cooled by IC scattering. However, we expect that the SED does not change significantly in the 10 keV $- 100$ MeV range, as shown in Sotomayor Checa et al. (2021).

5. Conclusions

We have modeled a PopIII super-Eddington microquasar, where a super-critical accretion disk launches winds, which help to maintain the accretion rate at the Eddington limit in the inner part of the disk. These winds collide with a powerful jet that deflects them, generating an equatorial supersonic flow which interacts with the PopIII star. This interaction allows the formation of shocks causing the acceleration of particles, and non-thermal high energy emission is produced via IC scattering. We conclude that the equatorial winds are able to produce hard X-rays and gamma rays in microquasars from the early universe.

References

Abramowicz M.A., Calvani M., Nobili L., 1980, ApJ, 242, 772
Eichler D., Usov V., 1993, ApJ, 402, 271
Fukue J., 2004, PASJ, 56, 569
Lee H.M., Kang H., Ryu D., 1996, ApJ, 464, 131
Narayan R., Yi I., 1994, ApJL, 428, L13
Shakura N.I., Sunyaev R.A., 1973, A&A, 500, 33
Sotomayor Checa P., Romero G.E., 2019, A&A, 629, A76
Sotomayor Checa P., Romero G.E., Bosch-Ramon V., 2021, Ap&SS, 366, 13
Wang J.M., Zhou Y.Y., 1999, ApJ, 516, 420